Water Resources Research

Supporting Information for

Stormflow response and 'effective' hydraulic conductivity of a degraded tropical *Imperata* grassland catchment as evaluated with two infiltration models

Zhuo Cheng[1,2], Jun Zhang[3,4,*], Bofu Yu[2], Nick A. Chappell[5],

H.J. (Ilja) van Meerveld[6], and L. Adrian Bruijnzeel[3,7]

[1]Department of Geography, Beijing Normal University, Beijing, P. R. China

[2]Australian Rivers Institute and School of Engineering and Built Environment, Griffith University, Brisbane, Australia

[3]Institute of International Rivers and Eco-Security, Yunnan University, Kunming, P. R. China

[4]Environmental Modelling, Sensing & Analysis, TNO, Petten, The Netherlands

[5]Lancaster Environment Centre, University of Lancaster, Lancaster, United Kingdom

[6]Department of Geography, Hydrology and Climate, University of Zurich, Zurich, Switzerland

[7]Department of Geography, King's College London, London, United Kingdom

Contents of this file

Introduction

Supporting text S1 provides additional evidence regarding the dominance of infiltration-excess overland flow at the study site. Supporting Figure S1 graphically illustrates the conceptual difference between the two infiltration models employed in the study (GA and SVI) whereas Supporting Figures S2–S4 present additional examples of the comparative performance of the GA and SVI models for different types of storm events. The remaining Supporting Figures present the temporal variability of the spatially averaged maximum infiltration parameter I_m in the SVI model (S5) as well as tentative relations between I_m (and initial abstraction loss, F_0) and soil bulk density / soil organic matter content (S6) or the 'effective' hydraulic conductivity in the GA model (S7).

Text S1.

Data-Based Mechanistic model application and evidence for stormflow runoff generation regime

The 157-mm rain event on 28–29 June 2013 produced a very flashy streamflow generation with a transfer time ('time constant') of the propagating flood wave (*i.e.,* celerities) through the catchment of 84 min. For this period in this catchment, the optimal model producing this time constant is a purely first-order linear model with no delay between rainfall and first streamflow response and a Nash-Sutcliffe simulation efficiency of 0.90. The rainfall to riparian pore-water response (regulated by a subsurface response) for this event was, however, considerably slower with a response time of 59 hours plus 5 min delay; this also had a first-order linear transfer function structure. An even more flashy time of response of only 16 min was produced for the smaller 55 mm event over the 3–5 July 2013 period. The optimal model structure identified was the same as for the 28–29 June event, though the simulation efficiency was lower (0.81). Again, the response of the riparian pore-water level to rainfall was considerably slower at 417 hours plus 40 min delay between rainfall and initial piezometer response (Rt^2 0.90). The observations also demonstrated that streamflow peaked well before the riparian water-level (as observed in the piezometer) reached the ground surface. This observation, combined with the systems modeling, indicates that both periods (and others examined in the record), exhibit a response of the riparian subsurface that is considerably slower / more damped when compared with the streamflow, indicating that infiltration-excess overland flow is the dominant source of streamflow for these events at this locality. Indeed, the response time of only 16 min for the July storm is considerably more flashy than that observed for the similarly-sized South Creek Experimental Catchment in Queensland during the severe Category 4 Tropical Cyclone Joy (Chappell *et al.,* 2012), where saturation overland flow on the hillside was considered a dominant pathway (Bonell *et al.,* 1998).

Datasets	Period	Structure[1]		a[2]	b[3]	Rt[2] [4]	YIC[5]	TC[6]
Rain-streamflow	28-29/6/2013	[1 1 0]	-0.9423	0.0263	0.90052	-4.272	84.07 min	
Rain-streamflow	3-5/7/2013	[1 1 1]	-0.7419	0.0897	0.81209	-6.396	16.75 min	
Rain-porewater	28-29/6/2013	[1 1 1]	-0.9986	0.6049	0.92218	-6.496	59.28 hours	
Rain-porewater	3-5/7/2013	[1 1 8]	-0.9998	0.7128	0.90420	-9.978	417.10 hours	

[1] transfer function model structure given in form of [number of denominators; number of numerators; number of pure time delays];

[2] The value of the 'a' or recession parameter identified for a first-order discrete time transfer function model;

[3] The value of the 'b' or gain parameter identified for a first-order discrete time transfer function model;

[4] Simplified Nash-Sutcliffe simulation efficiency (R_t^2);

[5] Young Information Criterion (YIC);

[6] Time constant of the identified first-order, discrete-time transfer function model derived from the 'a' parameter and data time-step. See Chappell *et al.* (1999) for explanations.

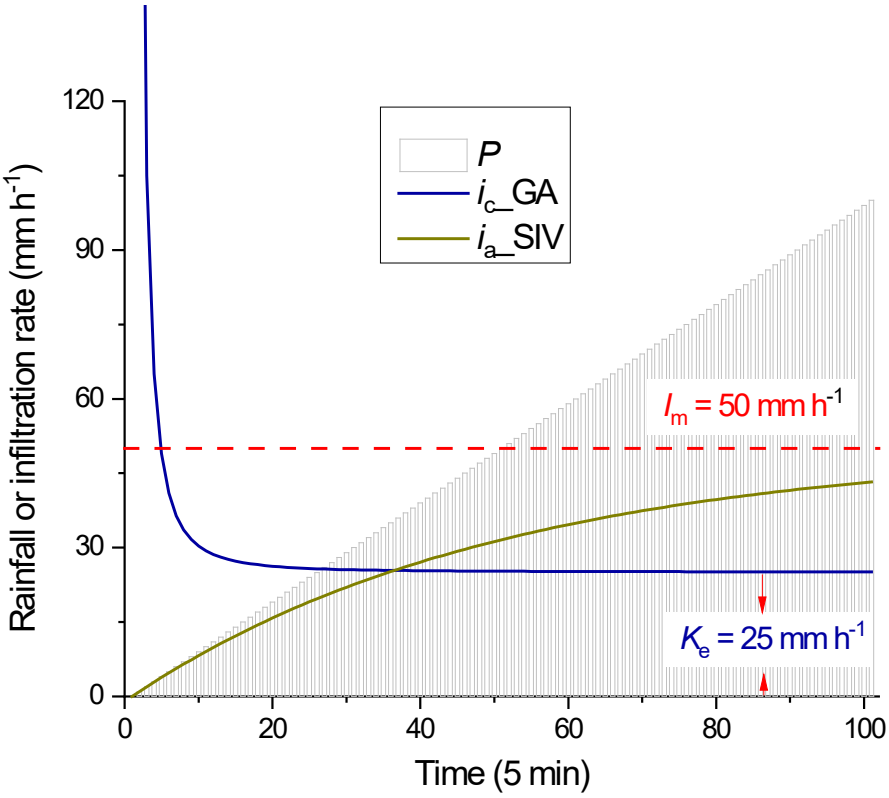

Figure S1. Illustration of the different ways in which the infiltration process is modeled by the GA and SVI models for an event with a linearly increasing rainfall intensity: i_c_GA is the infiltration capacity as derived by GA for K_e= 25 mm h^{-1} and ψ_m = 0.8 mm; i_a_SVI denotes the actual infiltration rate according to SVI for F_0 =10 mm and I_m = 50 mm h^{-1}.

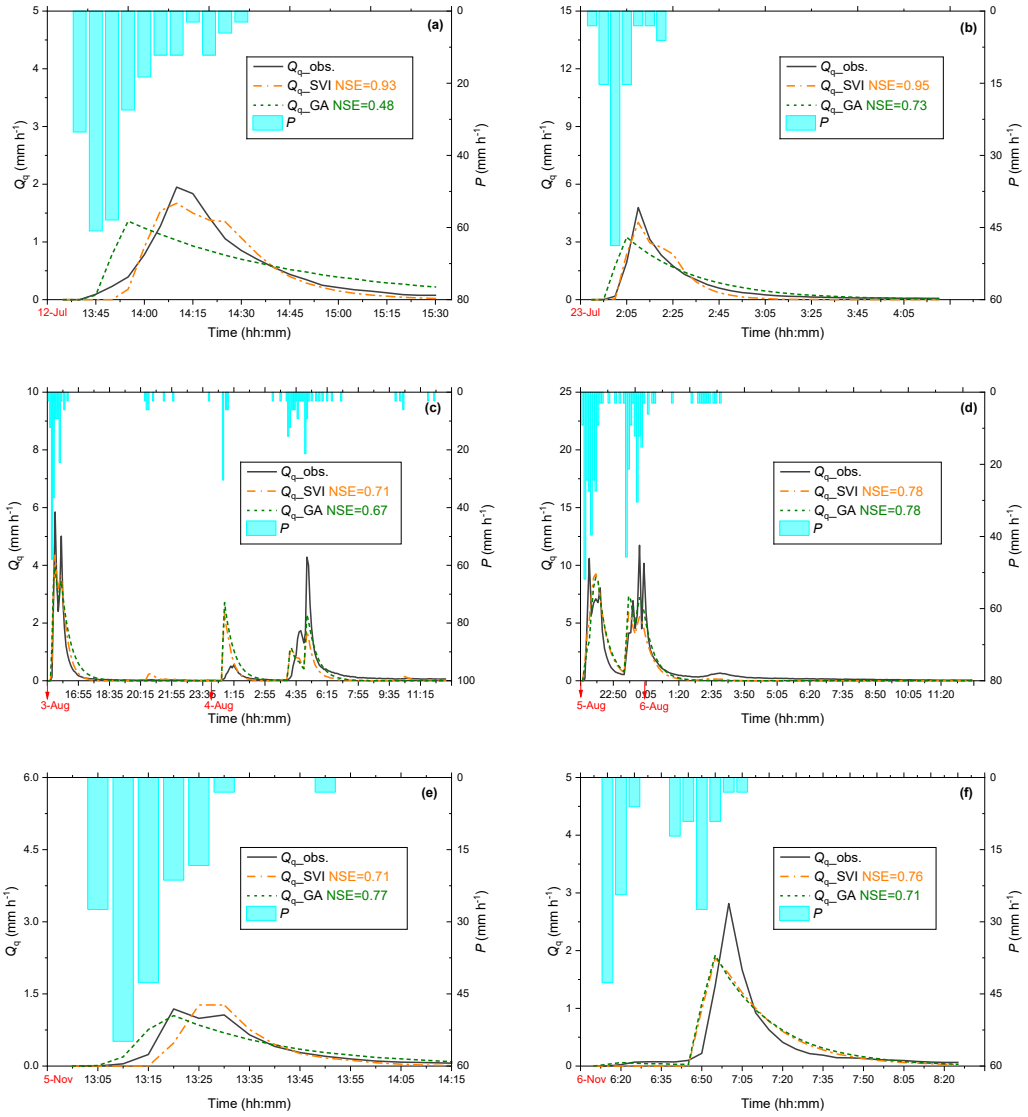

Figure S2. Comparison of observed and predicted hydrographs by GA and SVI for selected storm events. NSE = Nash-Sutcliffe efficiency value.

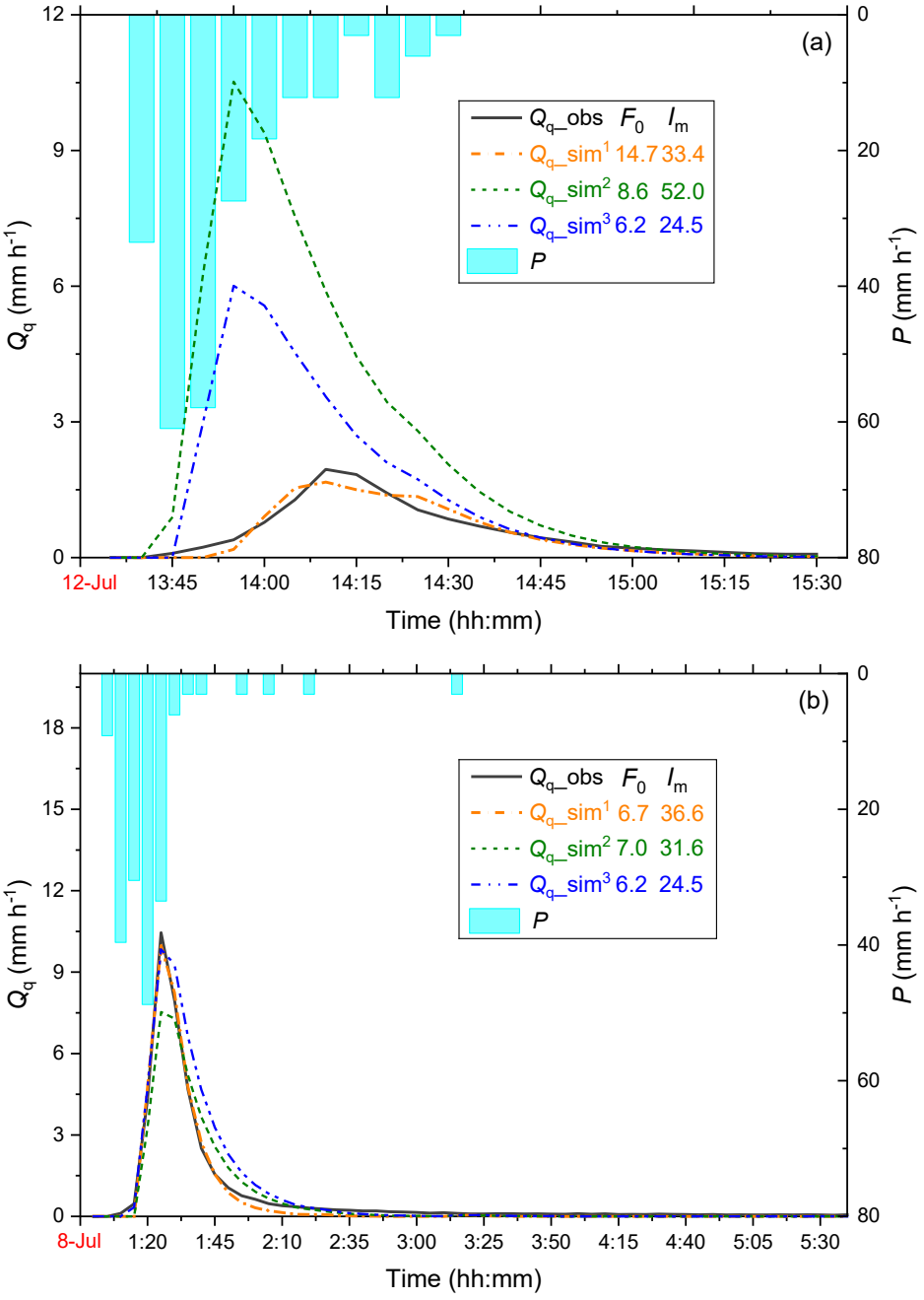

Figure S3. Comparison of observed (Q_q_obs) and predicted (Q_{q_sim}) hydrographs by SVI in three modes, *i.e.* with both parameters calibrated (Q_q_sim^1); with median values of calibrated parameters for all 30 events (Q_q_sim^2); and with parameters derived from SWC_{10}. Panel **(a)** represents the highest discrepancy in performance for the three predictions (event of 12 July 2013, 20.6 mm of rain, storm runoff coefficient (R_c) of 5%), and panel **(b)** the lowest discrepancy (event of 8 July 2013, 15.5 mm, R_c = 21%).

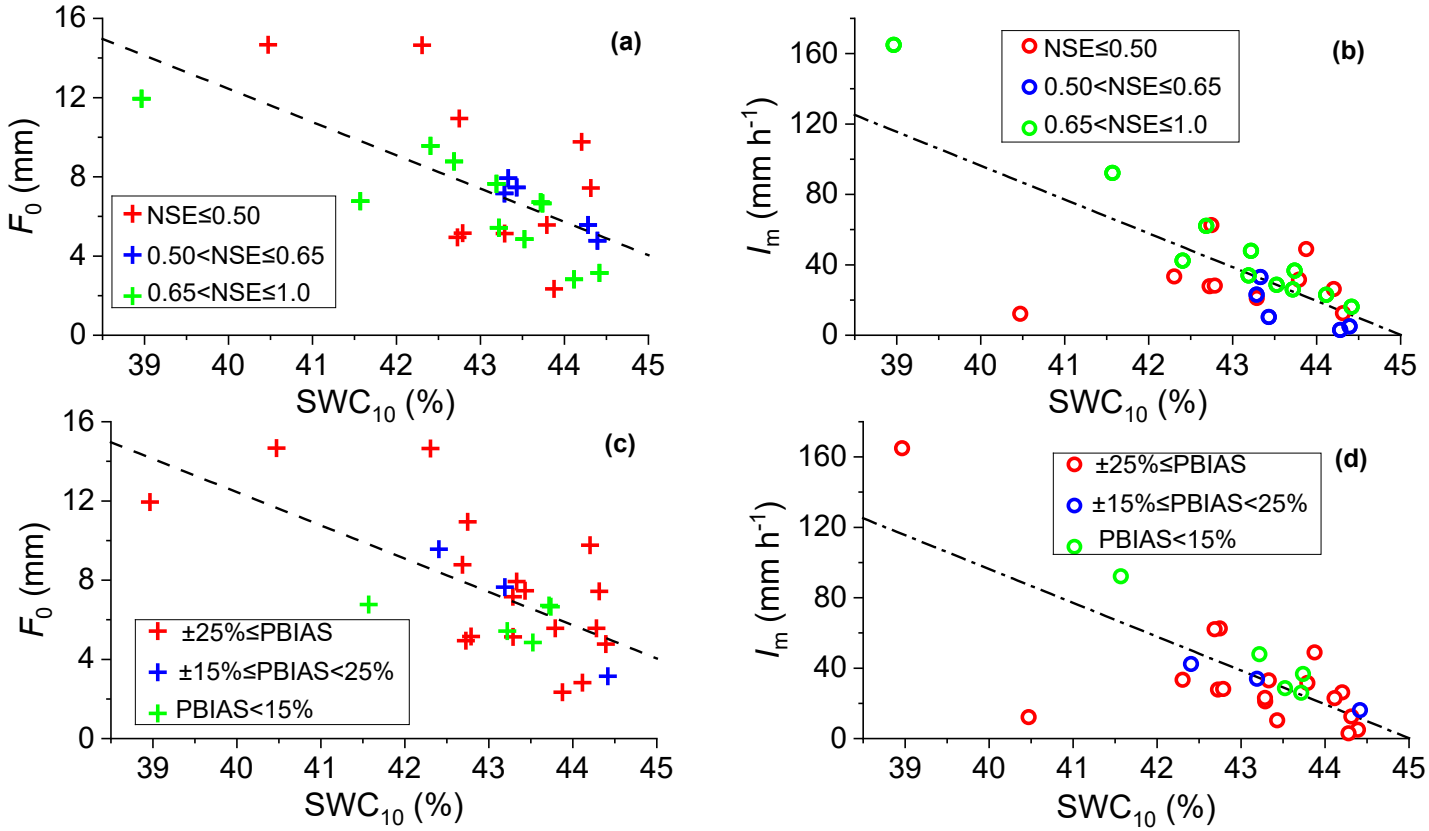

Figure S4. Relations between mid-slope soil moisture content at 10 cm (SWC_{10}) and the calibrated values of initial abstraction, F_0 and the spatially average maximum infiltration capacity, I_m for 26 events; points are colour-coded by the class of **(a) & (b)** Nash-Sutcliffe efficiency, NSE and **(c) & (d)** the ratio of the simulated to the observed event total stormflow (PBIAS) for the simulations using predicted values of F_0 and I_m (dashed lines).

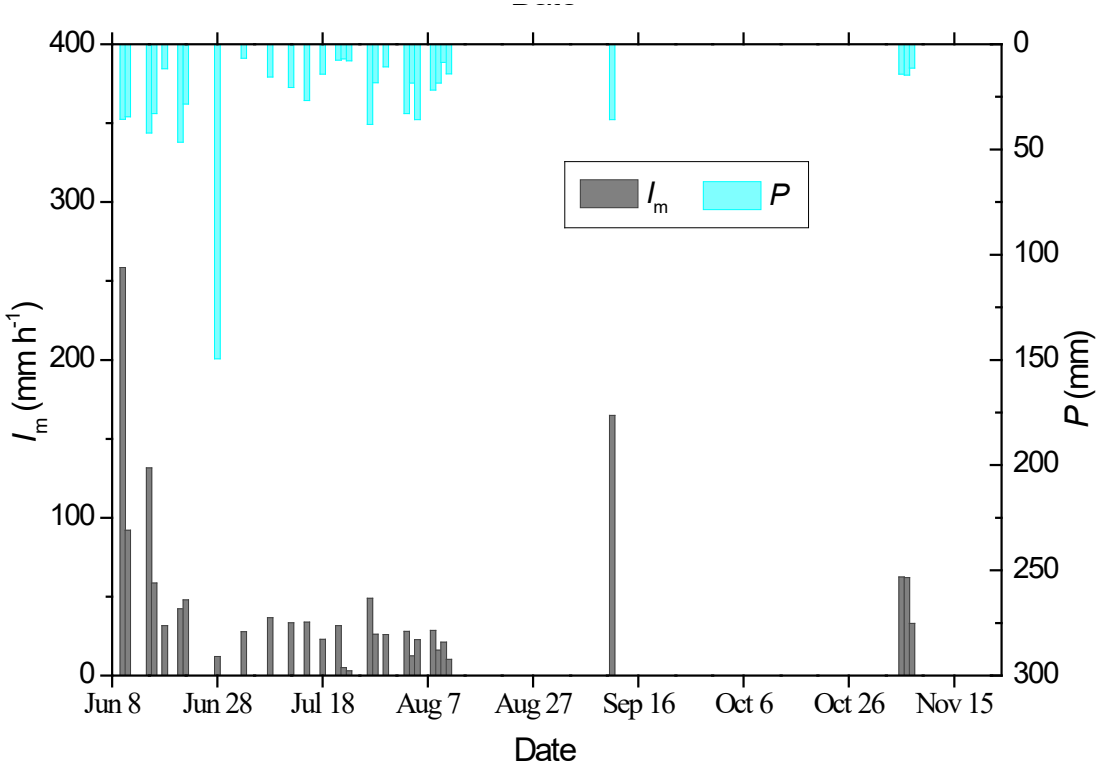

Figure S5. Temporal variability of the spatially averaged maximum infiltration capacity I_m as derived for each individual runoff event between 8 June and 7 November 2013.

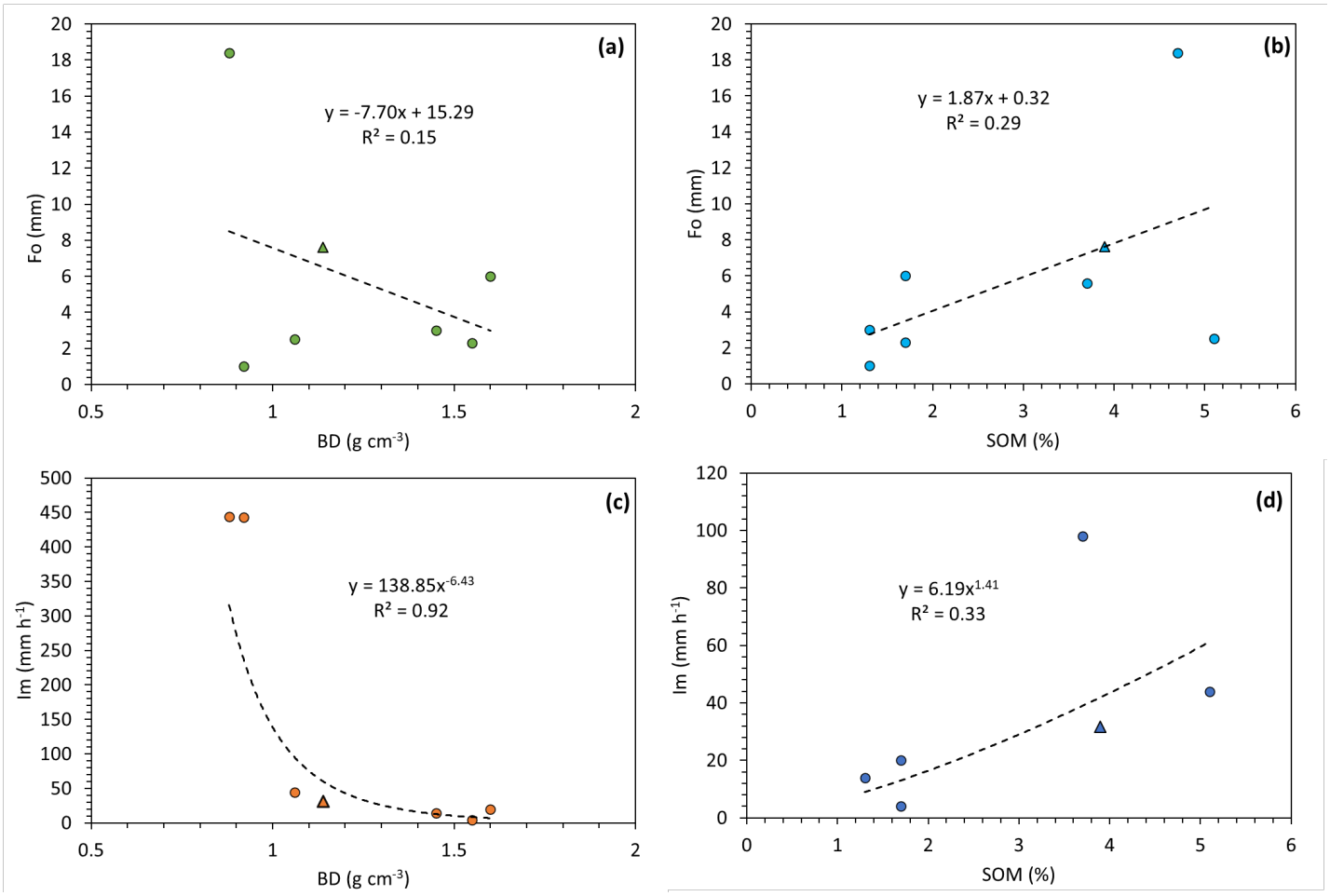

Figure S6. Tentative relationships between **(a)** soil bulk density (BD, g cm$^{-3)}$ and **(b)** soil organic matter content (SOM, %) and initial abstraction, F_0 (mm); and between **(c)** BD and **(d)** SOM and the spatially averaged maximum infiltration rate (I_m, mm h^{-1}) as measured at various sites in Southeast Asia (Yu *et al.*, 1997b; Coughlan, 1997; Van Dijk & Bruijnzeel, 2004). Data for the Basper grassland indicated by triangle.

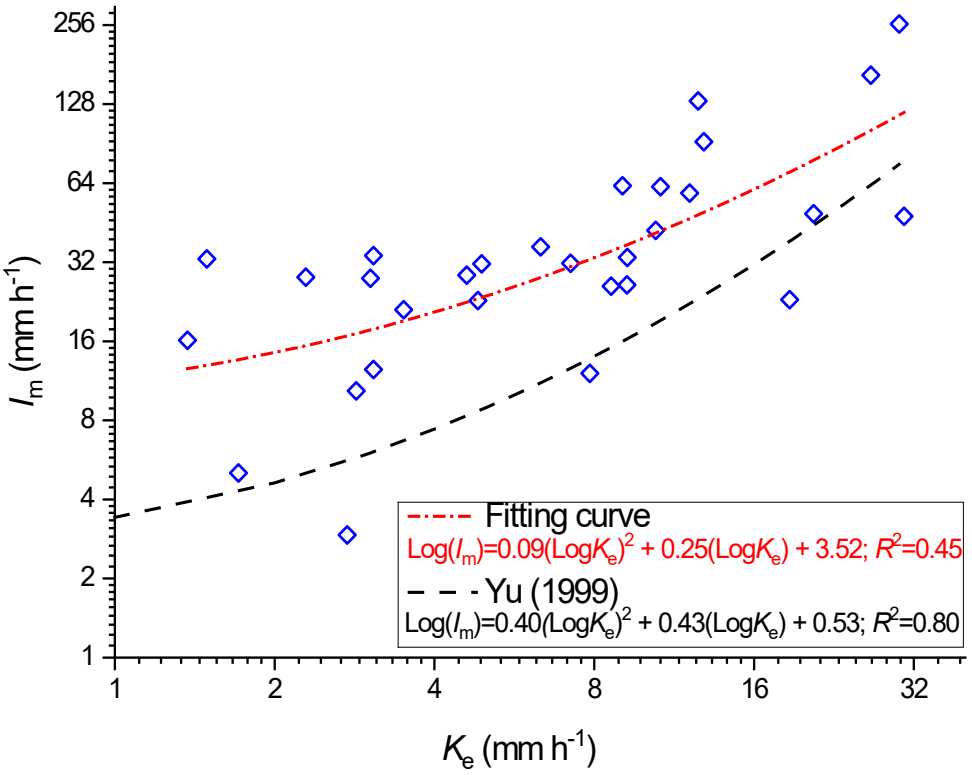

Figure S7. Relationship between Log(I_m)- and Log(K_e)-values derived for each of the 30 examined runoff events at the Basper grassland. Second-order polynomial equation derived by Yu (1999) for six sites in Southeast Asia and Queensland added for comparison.